Quantitative Determination of Band Distortions in Diamond Attenuated Total Reflectance Infrared Spectra

Maxime Boulet-Audet,[†] Thierry Buffeteau,[§] Simon Boudreault,[‡] Nicolas Daugey,[§] and Michel Pézolet*[,†]

Centre de Recherche sur les Matériaux Avancés CERMA, Département de Chimie, and Département de Biologie, Université Laval, Pavillon Alexandre-Vachon, Québec G1 V 0A6, Canada, and Institut des Sciences Moléculaires, UMR 5255 du CNRS, Université de Bordeaux I, 33405 Talence, France

Received: February 26, 2010; Revised Manuscript Received: May 7, 2010

Due to its unmatched hardness and chemical inertia, diamond offers many advantages over other materials for extreme conditions and routine analysis by attenuated total reflection (ATR) infrared spectroscopy. Its low refractive index can offer up to a 6-fold absorbance increase compared to germanium. Unfortunately, it also results for strong bands in spectral distortions compared to transmission experiments. The aim of this paper is to present a methodological approach to determine quantitatively the degree of the spectral distortions in ATR spectra. This approach requires the determination of the optical constants (refractive index and extinction coefficient) of the investigated sample. As a typical example, the optical constants of the fibroin protein of the silk worm *Bombyx mori* have been determined from the polarized ATR spectra obtained using both diamond and germanium internal reflection elements. The positions found for the amide I band by germanium and diamond ATR are respectively 6 and 17 cm^{-1} lower than the true value dtermined from the $k(\nu)$ spectrum, which is calculated to be 1659 cm^{-1}. To determine quantitatively the effect of relevant parameters such as the film thickness and the protein concentration, various spectral simulations have also been performed. The use of a thinner film probed by light polarized in the plane of incidence and diluting the protein sample can help in obtaining ATR spectra that are closer to their transmittance counterparts. To extend this study to any system, the ATR distortion amplitude has been evaluated using spectral simulations performed for bands of various intensities and widths. From these simulations, a simple empirical relationship has been found to estimate the band shift from the experimental band height and width that could be of practical use for ATR users. This paper shows that the determination of optical constants provides an efficient way to recover the true spectrum shape and band frequencies of distorted ATR spectra.

Introduction

Infrared transparent materials like germanium, silicon, zinc sulfur, KRS-5 (thallium iodide and chloride), zinc selenide, and diamond are generally used as internal reflection elements (IRE) for attenuated total reflection infrared spectroscopy.[1] The physical properties of these materials undoubtedly affect their use as ATR accessories. For example, the lower the refractive index of the material, the deeper the evanescent wave and the higher the absorbance.[2] Therefore, small bands due to weakly absorbing vibrations or to small sample size such as fibers can be substantially increased while using a lower refractive index IRE. Since its first application as an IRE,[3] diamond has been increasingly used for routine ATR spectroscopy because it is the hardest material, chemically inert, nontoxic, and can withstand very high pressures. Several diamond ATR accessories are currently commercially available and have been used to study various inorganic,[4−6] organic,[7−9] and biological[10−14] systems.

Due to the nature of ATR measurements, the observed spectra can be strongly affected (band positions and relative intensities) by the anomalous dispersion (AD) of the refractive index of the absorbing sample, which can be problematic for quantitative as well as qualitative analysis. For instance, shifted bands could be assigned to wrong vibrational modes based on literature transmission data. For the particular case of proteins, a shift of the frequency of the amide I mode leads inevitably to an error in the determination of the secondary structure content. The intensity ratio between two bands can also be strongly altered by the use of a low refractive index IRE, especially if the bands are not well-resolved.[1] Consequently, an inaccurate determination of the intensity ratio of the amide I and amide II bands can result in a misleading interpretation of the orientation of proteins.

Transmittance spectra are essentially governed by the extinction coefficients of the sample (k), but they can be slightly affected by the refractive index (n) of the sample for very thin films with high oscillator strengths.[15] On the other hand, reflectance spectra are much more affected by the AD of the refractive index of the sample when the incidence angle is close to the critical angle or for strong absorption bands. These differences have been described theoretically by Hansen et al.[16] More recently, AD effects have been reported for polymers,[8,17] proteins,[18] and inorganic compounds.[6,19−22] Goormaghtigh et al.[1] have discussed qualitatively some AD effects in specific cases, especially the impact of the incidence angle, absorption coefficient, film thickness, and overlapping bands. However, the quantitative determination of the spectral distortions due to AD

* To whom correspondence should be addressed. E-mail: michel.pezolet@chm.ulaval.ca.
[†] Département de Chimie, Université Laval.
[‡] Département de Biologie, Université Laval.
[§] Université de Bordeaux I.

10.1021/jp101763y © 2010 American Chemical Society
Published on Web 05/27/2010

requires the full determination of the optical constants of the system under study.

The scope of this paper is to present a methodological approach to determine quantitatively the degree of the spectral distortions in ATR spectra and to propose a parctical way to estimate the band shifts due to AD. Spectral simulations have thus been performed using variable parameters to quantify their impact on the absorption bands. Spectra can be simulated for given experimental conditions (polarization, angle of incidence, etc.) using Fresnel's coefficients and the optical constants (refractive index $n(\nu)$ and extinction coefficient $k(\nu)$) of each layer forming the studied system.[23,24] To that end, the silk fibroin from the silkworm *Bombyx mori*[25−28] has been used as a model protein system. Like any other protein, this fibrous protein has strong and broad amide bands that are likely to be distorted in reflectance spectra. Due to its plasticity, silk fibroin does not need any sort of plasticizer to form solid homogeneous thick films, which is important for the accurate determination of the optical constants. For the first time, the optical constants of films of fibroin cast from the highly concentrated fibroin solution found in the silk gland have been determined from the data obtained using both diamond and germanium internal reflection elements. From these optical constants, spectral simulations have been performed to recover quantitatively the true position, shape, and intensity from distorted protein amide bands obtained by ATR spectroscopy. Spectral simulations have also revealed that the film thickness and the protein concentration are crucial parameters to control in order to reduce the AD effect. Furthermore, to extend this study to any systems, the ATR distortion amplitude has been evaluated using spectral simulations performed for bands of various intensities and widths. From these simulations, a simple empirical relationship has been found to estimate the band shift from the experimental band height and width.

Experimental Methods

Sample Preparation. The *Bombyx mori* silkworms were provided from the Feeder Factory (Mississauga, Canada). The worms were fed with a mulberry diet until they begin to produce silk filaments for their cocoon. They were dissected at their final stage in a phosphate buffer solution of pH 6.6. The silk glands were extracted and cleaned for 15 min with distilled water. To prevent the contamination of fibroin from sericin, the gland epithelium was perforated in its posterior part where sericin is not present, thus providing pure fibroin.[25] For ATR experiments, the fibroin was washed with distilled water and then placed on the IRE. The thick film was dehydrated with a gentle dry air flow until the protein absorbance reached its maximum while that of water was minimized. It seems that drying does not affect the fibroin conformation, as seen with the major ampullate silk dope of spiders,[29] so that the spectrum of the dried fibroin obtained can be considered as truly representative of the native cocoon silk.

Due to the high extinction coefficient of the amide bands of fibroin, the films used for transmission experiments have to be very thin in order to prevent the complete beam extinction in the region of interest. As strain forces can induce the formation of β-sheets,[27,30−32] squeezing the liquid silk was avoided to form thin films. Instead, thin films were cast from a dilute solution of solubilized silk. To this end, the doped solution of the gland was solubilized in a 5 M guanidium hydrochloride solution before removing the salt using a PD-10 desalting column (GE Healthcare Bio-Sciences AB, Björkgatan, Sweden). Subsequently, the films were prepared by casting the unsalted diluted solution on a BaF_2 window. However, some evidence suggests that the solubilization is not a perfectly conservative process as the rheological[26] and dynamic light-scattering behavior[33] of silk fibroin can be slightly affected by this treatment. Thus, solubilization may also modify the secondary structure of the fibroin. Because of this uncertainty, the transmittance spectrum will be shown for comparison, but the true frequency of the amide I band maximum will be that given by the more reliable optical calculation.

Spectral Acquisition and Treatment. All spectra were recorded with a Nicolet Magna 850 Fourier transform infrared spectrometer (Thermo Scientific, Madison, WI) equipped with a liquid-nitrogen-cooled narrow-band MCT detector using either Golden-Gate (diamond IRE) or Silver-Gate (germanium IRE) ATR accessories (Specac Ltd., London, U.K.). Both accessories were used with the smallest available aperture (0.75 mm) of the spectrometer and an angle of incidence θ of 45°. In the Golden-Gate apparatus, the infrared beam is focused with 4× magnification ZnSe lenses to a 190 μm diameter on the crystal, while for the Silver-Gate accessory, the beam diameter is about 750 μm without lenses. The electric field of the infrared beam was polarized either perpendicular (s) or parallel (p) to the plane of incidence with a ZnSe wire grid polarizer (Specac Ltd., London, U.K.). Each spectrum was obtained from the acquisition of 64 scans at 4 cm^{-1} resolution from 4000 to 750 cm^{-1} using a Happ−Genzel apodization. Experiments were carried out several times to obtain at least three spectra of dried silk with the maximum intensity. This condition is only obtained for a thick dry film covering the entire beam spot. All spectral operations were executed using the GRAMS/AI 8.0 software (Thermo Galactic, Salem, NH). The spectra were neither smoothed nor deconvolved. The only applied correction was an offset baseline at 4000 cm^{-1}. The exact peak positions were determined using the center of gravity of the 20% upper part of the band.[34]

Spectral Simulations. The computer program used to calculate the ATR spectra is based on the Abeles' matrix formalism,[35,36] which has been generalized for anisotropic layers.[37] Several parameters must be fixed in the program such as the number of layers (set to 1), the number of reflections (set to 1), the angle of incidence (set to 45°), the IRE refractive index (2.38 and 4.00 for diamond and germanium, respectively), and the polarization of the infrared beam (p or s). The anisotropic optical constants (refractive index and extinction coefficient in the three space directions) of the sample have to be determined beforehand (see the following paragraph). Because the sample preparation method does not induce orientation in the *xy* plane, a uniaxial symmetry of orientation can be assumed for the calculations ($n_x = n_y = n_{x,y}$ and $k_x = k_y = k_{x,y}$). Calculations were performed for sample thicknesses larger than the penetration depth of the infrared beam, so that the flatness of the protein film and the knowledge of its thickness were not essential in this study.

The spectral simulations of diluted samples were performed for concentration ranging from 0 to 100% (w/w) using the optical constants of fibroin calculated from the experimental ATR spectra and those of water calculated by Bertie et al.[38] The heterogeneous optical constants of the system have been calculated by simply averaging the $k(\nu)$ of pure constituents proportionally to their relative concentration before executing a Kramers−Kronig transform on the mixed $k(\nu)$ to calculate the related $n(\nu)$. This procedure assumes that there is no interaction between the protein and water.

Spectral simulations of bands of various widths and intensities were performed using the Abeles formalism for different $n(\nu)$ and $k(\nu)$ pairs. The extinction coefficient $k(\nu)$ was associated with a Lorentzian band initially positioned at 1650 cm^{-1} with a given width and intensity, whereas the refractive index $n(\nu)$ was calculated by the Kramers−Kronig transform of $k(\nu)$ using n_∞ of 1.5.

Determination of Optical Constants. The optical constants can be determined from only one experiment, such as ATR or transmittance at normal incidence, using the interdependence of $n(\nu)$ and $k(\nu)$ by the Kramers−Kronig relations.[39−45] The transmission method is particularly valuable for weak and moderately strong bands, whereas the ATR method can be applied to strong bands using a correction algorithm developed by Dignam et al.[44] In this study, the ATR method has been used due to the high oscillator strengths of amide I and amide II bands and because it does not require the use of thin films of uniform thickness.

In the case of s-polarized ATR experiments, Dignam et al have shown that the phase change spectrum $\delta_s(\nu)$ is given by the relationship[44]

$$\delta_s(\nu_a)=I_s - \frac{2}{\pi}P\int_0^\infty \frac{\nu \cdot \ln\sqrt{R_s(\nu)}}{\nu^2 - \nu_a^2}\,d\nu \quad (1)$$

with

$$I_s = 2\arctan\frac{\sqrt{n_0^2\sin^2\theta - n^2(\nu_u)}}{n_0\cos\theta} \quad (2)$$

where n_0 is the crystal refractive index, θ the angle of incidence, and $n(\nu_u)$ the refractive index in a region of constant reflectance at high wavenumber. From the experimental s-polarized ATR spectrum and the phase angle calculated using eqs 1 and 2, the complex Fresnel coefficient $\hat{r}_s(\nu) = [R_s(\nu)]^{1/2}\exp[i\delta_s(\nu)]$ can be calculated. This, in turn, allows direct calculation of the refractive index and extinction coefficient from the following equations

$$n(\nu) = n_0\,\mathrm{Re}\left[\sin^2\theta + \left(\frac{1-\hat{r}_s(\nu)}{1+\hat{r}_s(\nu)}\right)^2\cos^2\theta\right]^{1/2} \quad (3)$$

$$k(\nu) = -n_0\,\mathrm{Im}\left[\sin^2\theta + \left(\frac{1-\hat{r}_s(\nu)}{1+\hat{r}_s(\nu)}\right)^2\cos^2\theta\right]^{1/2} \quad (4)$$

It is noteworthy that this method, using an s-polarized ATR spectrum, allows the determination of the isotropic optical constant of the sample having its thickness higher than the penetration depth, d_p (i.e., 4000 Å and 1.2 μm at 1650 cm^{-1} for germanium and diamond crystals, respectively). For anisotropic samples exhibiting a uniaxial orientation, the in-plane optical constants ($n_{x,y}$ and $k_{x,y}$) can be calculated with the same procedure, whereas the out-of-plane optical constants (n_z and k_z) can be calculated from the p-polarized ATR spectrum using a similar theoretical approach. Indeed, for p-polarized ATR experiments, the phase change spectrum $\delta_p(\nu)$ is given by the relationship[44]

$$\delta_p(\nu_a)=I_p - \frac{2}{\pi}P\int_0^\infty \frac{\nu \cdot \ln\sqrt{R_p(\nu)}}{\nu^2 - \nu_a^2}\,d\nu \quad (5)$$

with

$$I_p = 2\arctan\frac{n_0\sqrt{n_0^2\sin^2\theta - n_z^2(\nu_u)}}{n_{x,y}(\nu_u)n_z(\nu_u)\cos\theta} \quad (6)$$

From the experimental p-polarized ATR spectrum and the phase angle calculated using eqs 5 and 6, the complex Fresnel coefficient $\hat{r}_p(\nu) = [R_p(\nu)]^{1/2}\exp[i\delta_p(\nu)]$ can be calculated. This complex Fresnel coefficient is directly related to the complex out-of-plane dielectric constant by the relation

$$\hat{\varepsilon}_z(\nu) = \frac{n_0^2\sin^2\theta}{\left[1 - \left(\frac{\hat{\varepsilon}_{x,y}(\nu)}{n_0^2}\right)\cdot\left(\frac{1-\hat{r}_p(\nu)}{1+\hat{r}_p(\nu)}\right)^2\cos^2\theta\right]} \quad (7)$$

where $\hat{\varepsilon}_z(\nu) = \varepsilon'_z(\nu) + i\varepsilon''_z(\nu) = (n_z(\nu) + ik_z(\nu))^2$

The refractive index $n_z(\nu)$ and extinction coefficient $k_z(\nu)$ can be extracted from the complex out-of-plane dielectric constant $\hat{\varepsilon}_z(\nu)$ using the following equations

$$n_z(\nu) = \sqrt{0.5(\sqrt{\varepsilon'^2_z(\nu) + \varepsilon''^2_z(\nu)} + \varepsilon'^2_z(\nu))} \quad (8)$$

$$k_z(\nu) = \sqrt{0.5(\sqrt{\varepsilon'^2_z(\nu) + \varepsilon''^2_z(\nu)} - \varepsilon'^2_z(\nu))} \quad (9)$$

Results and Discussion

Figure 1 shows the s-polarized spectra of silk fibroin obtained by diamond and germanium ATR and by transmission spectroscopy. The wavenumber position of the amide I and amide II bands of the transmittance spectrum is typical of unordered and/or helical proteins, in agreement with the literature.[31,46−48] The spectrum obtained by germanium ATR is very close to the transmittance spectrum, while the spectrum obtained by diamond ATR is quite different. Since the amide I band is the most extensively studied and the most intense band of a protein, it is interesting to investigate its behavior as a function of the experimental conditions. Several parameters could have been chosen to quantify the band asymmetry,[49] but the frequency at the maximum can describe more intuitively the amplitude of the distortion caused by the AD effect.

The amide I band maximum, located at 1642 cm^{-1} in the diamond ATR spectrum, is dramatically shifted toward low frequencies as compared to the transmittance spectrum (1656 cm^{-1}). Using germanium IRE, even if it is smaller, the red shift is still significant (1652 cm^{-1}). In addition, the amide I/amide II band intensity ratio, $I_{\text{amide I}}/I_{\text{amide II}}$, changes from 0.96 for diamond to 1.32 for germanium ATR. This difference is due to the fact that the refractive index increases in the vicinity of absorption bands as the frequency decreases. Consequently, the refractive index in the amide II region that is located on the low wavenumber side of the amide I band is higher and closer to that of diamond, making the amide II band more affected by the AD of the refractive index than the amide I band.[1,2] The interpretation of diamond ATR spectra can be significantly biased due to band shift and erroneous relative intensity. For

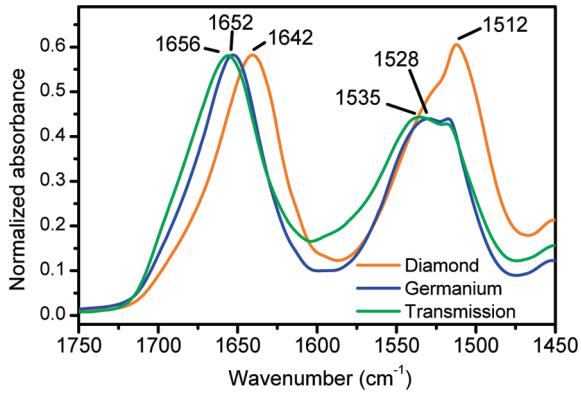

Figure 1. Transmittance spectrum and s-polarized diamond and germanium ATR spectra of a *B. mori* silk fibroin film. The spectra were normalized so that the peak heights of the amide I bands were equal. The germanium ATR spectrum has been multiplied by 5.98 with respect to diamond ATR.

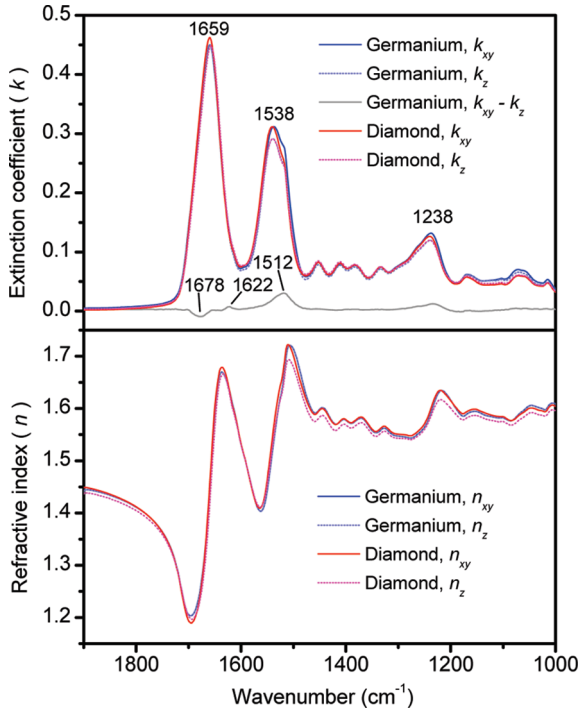

Figure 2. Fibroin optical constants calculated from germanium and diamond ATR.

an accurate interpretation, it is necessary to recover the true shape of absorption bands by determining the extinction coefficient of the system.

Determination of the Optical Constants of Silk Fibroin Using ATR. Figure 2 shows the calculated optical constants of pure native fibroin films thicker than the penetration depth ($d \gg d_p$) from both germanium and diamond ATR spectra. When using n_∞ of 1.52, a value close to that determined in the literature,[50,51] the optical constants determined from the ATR spectra obtained using the two IRE are in very good agreement with each other, which suggests that the method provides accurate optical constants $n(\nu)$ and $k(\nu)$. As expected, being governed by the Kramers−Kronig relation, the $n(\nu)$ spectrum follows the $k(\nu)$ spectrum with a derivative shape when crossing the absorption bands. Due to the cumulative effect of the AD, the $n(\nu)$ value rises as the wavenumber decreases. The $n(\nu)$ curve reaches a maximum of 1.72 at the top of the amide II band, which is slightly above the maximum value of 1.68 permitted

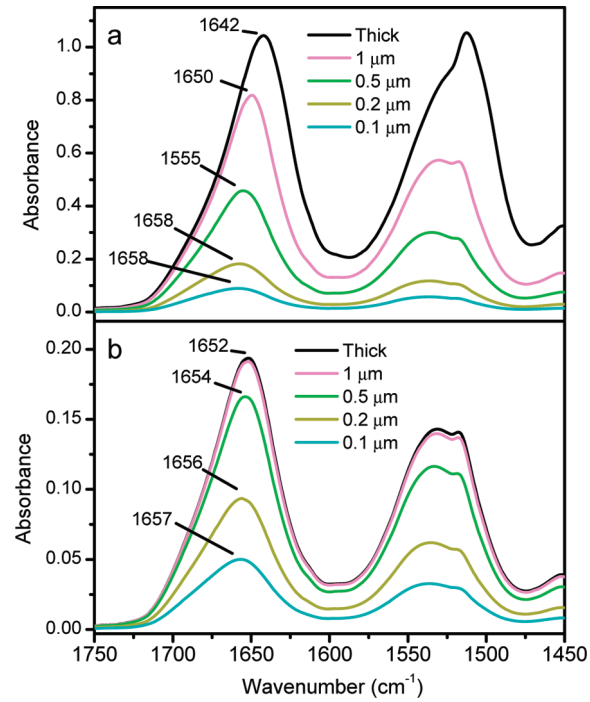

Figure 3. p-Polarized simulated (a) diamond and (b) germanium ATR spectra of silk fibroin of films of different thicknesses.

by the Snell law for diamond IRE. Above this value, the condition of total internal reflection is not respected since the critical angle θ_c is higher than the angle of incidence (i.e., 45°). Thus, it was predictable that strongly distorted amide I and amide II bands would arise when using a diamond IRE with an incident angle of 45°. To reduce this effect, the most obvious way is to make sure that θ is far enough from the critical angle θ_c, using for example a higher refractive index material instead of diamond, as shown in Figure 1.

The $k_{max} = 2k_{xy} + k_z$ values obtained for the amide I and II bands are 1.35 and 0.91, respectively, in good agreement with the values found in the literature for protein and peptides in the unordered and helical conformation.[12] In addition, the intensity ratio of the amide I and amide II bands, $I_{\text{amide I}}/I_{\text{amide II}}$, is 1.48, in agreement with the results usually obtained for globular proteins by transmission.[52] The true position of the amide I maximum of the silk fibroin structure is 1659 cm^{-1} as deduced from the extinction coefficient's maximum. This value is 7 cm^{-1} higher than the frequency observed in the germanium ATR spectrum and 17 cm^{-1} higher than that in the diamond ATR spectrum. The shift of the amide II maximum is even larger, 26 cm^{-1}, when using a diamond IRE. The fact that the calculated in-plane and out-of-plane extinction coefficients are almost identical indicates that the film is nearly isotropic. Nevertheless, the $k_{xy} - k_z$ spectrum reported in Figure 2 reveals two weak bands in the amide I and one in the amide II regions, indicating a small anisotropy of the sample. The 1678 cm^{-1} component can be assigned to turns and the 1622 cm^{-1} to β-sheets.[47,48,53]

Effect of the Sample Thickness. The impact of the sample thickness on the band distortions induced by ATR spectroscopy has been monitored by simulating p-polarized ATR spectra of silk fibroin films using the optical constants of Figure 2.

Figure 3 shows the diamond and germanium ATR simulated p-polarized spectra of silk fibroin films of different thicknesses. When thinning the sample, the absorbance decreases, while the position of the peak maximum increases. Because of the smaller penetration depth of germanium, a 1 μm fibroin film has nearly

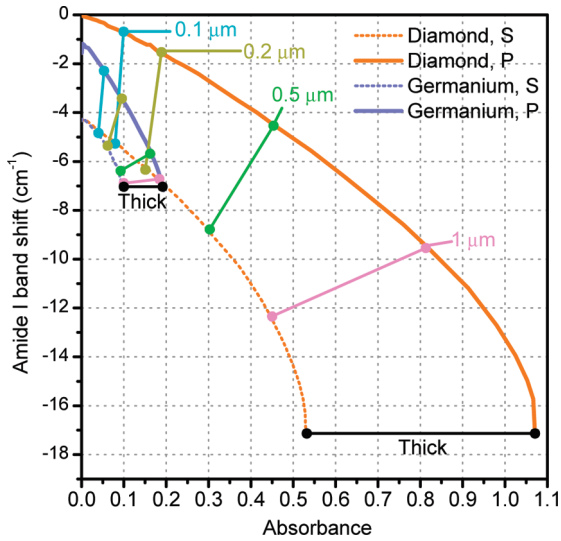

Figure 4. Wavenumber shift of the amide I band as a function of the maximum absorbance of the amide I for films of different thickness on diamond and germanium IRE. The dots on these curves joined by straight lines represent the shifts observed for p and s polarization for a given thickness from thin ($d \ll d_p$) to thick ($d \gg d_p$).

the same spectral signature as that of a thick film. However, for diamond ATR, thinning the sample down to 1 μm reduces the red shift of the amide I band by 8 cm^{-1} while sacrificing only 31% of the absorbance of the amide I band. Compared to a thick film, a 0.1 μm film has almost no spectral distortions, but the absorbance for diamond ATR is 12.7 and 3.8 fold lower for germanium ATR.

Figure 4 shows the effect of the absorbance on the position of the amide I band for the p and s polarization for diamond and germanium IRE. Starting from thick films, the shift is the same for both polarizations. As the film becomes thinner, both the absorbance and the shift for p polarization decrease faster. For the same film thickness, the curves also show that the p-polarized spectrum is always less shifted than the s-polarized one. When the film is thin enough, the shift of the amide I band of the p-polarized spectra becomes small. In addition, for the same film thickness, germanium ATR is less affected than diamond, but for the same absorbance values, diamond ATR spectra are less shifted. These spectral simulations clearly show that thinning the sample offers a fair compromise between signal lost and gained accuracy, especially for the p polarization.

Effect of Dilution. Since proteins are commonly investigated in aqueous solution (D_2O or H_2O), it is important to check the effect of dilution on spectral distortions. Indeed, it has been observed that even when the sample is diluted, strong absorption bands of ATR spectra can still be observed at lower frequency compared to transmittance spectra.[5,16] Fortunately, the excellent reproducibility of the sample thickness probed by the infrared beam (given by the penetration depth) makes the water subtraction easier by ATR than by transmission spectroscopy. Spectral simulations of protein and water mixtures have been carried out in order to estimate the AD effect observed for various dilute solutions.

Figure 5 shows the simulated amide I band of silk fibroin solutions at different concentrations after subtraction of the water contribution and the red shift of the amide I band induced by the AD of the refractive index. Results are presented only for the s polarization since for an isotropic thick film, $-\log R_s = -0.5 \log R_p$. As can be seen, even at 1% concentration, the amide I is significantly shifted toward low wavenumbers (6 cm^{-1}) with respect to the true position shown in Figure 2, and

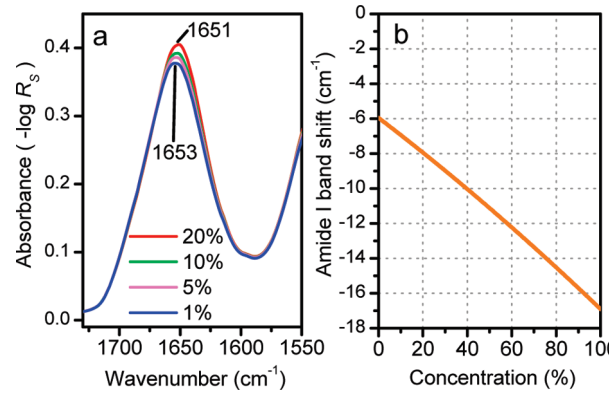

Figure 5. (a) s-Polarized diamond ATR spectra simulated in the amide I region for thick fibroin film at different concentrations after water subtraction and (b) an amide I band wavenumber shift as a function of the concentration. The spectra in panel (a) were normalized in intensity by dividing each spectrum by the protein weight fraction.

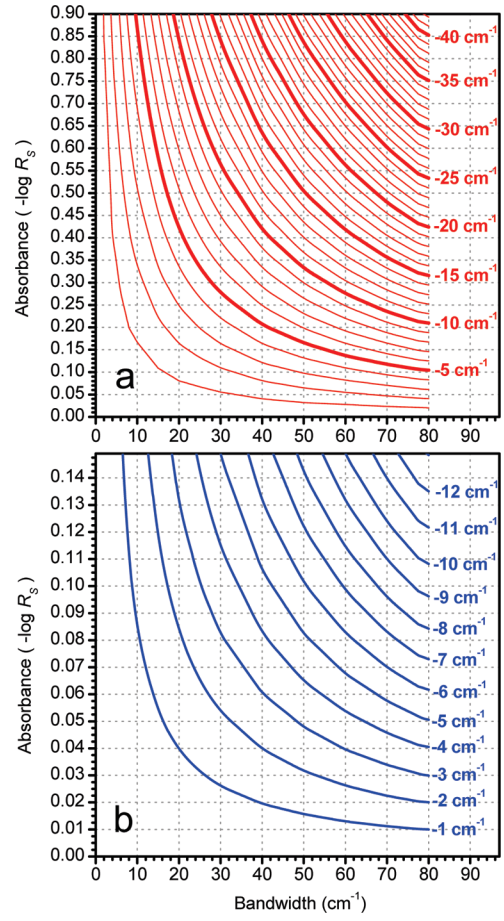

Figure 6. Constant ATR band shift curves for different values of the absorbance and bandwidth of a Lorentzian band. These curves were calculated from spectral simulations for s polarization using (a) diamond and (b) germanium as the internal reflection element.

the effect is the worst at higher concentration. Despite the fact that dilution does not solve entirely the AD effect issue, it can greatly improve the accuracy of any ATR measurements by reducing the refractive index of the solution.

Effect of the Extinction Coefficient and Band Shape. As seen above, using a diamond IRE for ATR experiments can lead to strong shifts of the infrared bands of highly absorbing materials. On the other hand, many systems have weaker and narrower bands, which would result in smaller AD effects and

TABLE 1: Predicted Band Shifts Using a Single Band Model for the Amide I Vibration of Silk Fibroin

IRE	experimental band position (cm^{-1})	experimental bandwidth (cm^{-1})	experimental band height ($-\log R_s$)	estimated band shift (± 0.1 cm^{-1})	estimated band position (± 0.1 cm^{-1})	true position of band k (cm^{-1})
diamond	1640.5	53	0.582	−18.5	1659.0	1659.3
germanium	1651.4	54	0.098	−6.3	1657.7	

red shifts. To estimate whether the observed shift can be neglected for a given thick film system, simulations have been performed for a single Lorentzian band as a function of width and maximum intensity (k_{max}). Various pairs of the optical constants $n(\nu)$ and $k(\nu)$ for values of k_{max} and bandwidths lower than 1.4 and 80 cm^{-1}, respectively, have been calculated using $n_\infty = 1.5$. Then, s-polarized ATR spectra were simulated, and the band shift (difference between the wavenumber of the calculated band maximum and that of the original Lorentzian band) was determined. We have found that the n_∞ value has little impact on the shift of the simulated band, especially for germanium ATR. In addition, the band shift is independent of the original frequency of the band in the mid-infrared spectral region.

As seen in Figure 6, the band shifts can be estimated using the bandwidth and the peak maximum absorbance. The figure clearly shows that the shift for a strong and broad band is more important for diamond ATR. A band with a given k_{max} and width will be more shifted by approximately 3 fold for diamond ATR compared to that for germanium ATR. For the same band area, broader bands will be the more shifted. Consequently, the band height and width must be considered independently. According to the curves of Figure 6, the shift varies almost linearly with either the bandwidth or the height of the band. As a result, the band shift can be related to the bandwidth and the maximum absorbance by a simple empirical relation

$$\text{band shift} = m*((-\log R_s) + b)*\text{bandwidth} \quad (10)$$

where m and b are constants valid for k_{max} values between 0 and 2. For diamond ATR, $m = -0.596 \pm 0.001$ and $b = 0.0031 \pm 0.0007$, while for germanium ATR, $m = -1.144 \pm 0.008$ and $b = 0.0037 \pm 0.0005$. Using eq 10 with the measured height and bandwidth values, the shift has been estimated for the amide I band of fibroin. The true position of the amide I band is the wavenumber value of the maximum k, as shown in Figure 2.

As seen in Table 1 for diamond and germanium ATR, the estimated band positions for the amide I band are in very good agreement with the true band positions, supporting the validity of the empirical relation eq 10. In the case of a sufficiently narrow and/or weak band, the shift due to the AD effect is very small, especially when using germanium ATR. The band shift can be lower than 1 cm^{-1} if the product of the bandwidth and height is lower than 1.6 for diamond ATR and 0.8 for germanium ATR.

Unfortunately, the curves in Figure 6 and eq 10 are only accurate for an isolated band and do not take into account the effect of a nearby band that could modify the band shape and enhance the band shift.[1,54] Nevertheless, they can be very useful to estimate the shift of the observed bands induced by the use of either diamond or germanium IRE. To avoid spectra misinterpretations, the estimation of the observed band shift is an easily applicable alternative to the complete correction of the spectra or the change of experimental parameters.

Conclusions

For the first time, the in-plane (xy) and out-of-plane (z) optical constants of dry native fibroin have been determined from diamond and germanium ATR spectra. These optical constants can be used as references for the extinction coefficient and refractive index of unordered proteins. Using the same approach, the optical constants of other proteins with different conformations could be determined. This study shows that the strong extinction coefficient of the amide I and amide II bands induced a significant anomalous dispersion effect when a low refractive index IRE like diamond was used. This effect is characterized by a shift toward low wavenumbers of the absorption bands in the ATR spectra. Using the values of $n(\nu)$ and $k(\nu)$ of fibroin, various simulations have been performed to determine the experimental conditions that would minimize such undesirable effects. Although it decreases the measured absorbance, thinning or diluting the sample in a lower refractive index solvent can be very helpful to minimize the optical effects, especially for p-polarized diamond ATR spectra. Nevertheless, staying away from the critical angle by choosing high refractive index IRE is still a simple and efficient method to obtain ATR spectra that are more similar to their transmittance counterparts. For weak bands with an absorbance value below 0.02 absorbance units, the spectral simulation showed than the shift will be lower than 1 cm^{-1}. Otherwise, for common refractive index materials, the shift can be easily estimated by knowing the width and the height of the distorted band.

Acknowledgment. This work was supported by grants from the Natural Sciences and Engineering Research Council (NSERC) of Canada, the Fonds Québécois de Recherche sur la Nature et les Technologies (FQRNT), and the Centre Québecois sur les Matériaux Fonctionnels (CQMF). M.B.-A. is grateful to FQRNT for the award of a graduate scholarship. The authors express their gratitude to Jean-François Rioux-Dubé, Mélanie Tremblay, and Sébastien Blanchette for their precious technical support. The authors thank the Feeder Factory that generously provided silkworms used for the extraction of silk fibroin.

References and Notes

(1) Goormaghtigh, E.; Raussens, V.; Ruysschaert, J. M. *Biochim. Biophys. Acta* **1999**, *1422*, 105.
(2) Harrick, N. J. *Internal Reflection Spectroscopy*; John Wiley & Sons: New York, 1967.
(3) Milosevic, M.; Sting, D.; Rein, A. *Spectroscopy* **1995**, *10*, 44.
(4) Bulgarevich, D. S.; Horikawa, Y.; Sako, T. *J. Supercrit. Fluids* **2008**, *46*, 206.
(5) Hansen, W. N.; Horton, J. A. *Anal. Chem.* **1964**, *36*, 783.
(6) Buffeteau, T.; Grondin, J.; Lassègues, J. C. *Appl. Spectrosc.* **2010**, *64*, 112.
(7) Endelmann, A.; Diewok, J.; Baena, J. R.; Lendl, B. *Anal. Bioanal. Chem.* **2003**, *376*, 92.
(8) Everall, N.; Bibby, A. *Appl. Spectrosc.* **1999**, *53*, 461A.
(9) Causin, V.; Marega, C.; Guzzini, G.; Marigo, A. *Appl. Spectrosc.* **2004**, *58*, 1272.
(10) Schmidt, M.; Wolfram, T.; Rumpler, M.; Tripp, C. P.; Grunze, M. *Biointerphases* **2007**, *2*, 1.
(11) Kazarian, S. G.; Chan, K. L. A. *Biochim. Biophys. Acta* **2006**, *1758*, 858.
(12) Boulet-Audet, M.; Lefèvre, T.; Buffeteau, T.; Pézolet, M. *Appl. Spectrosc.* **2008**, *62*, 956.
(13) Garside, P.; Lahlil, S.; Wyeth, P. *Appl. Spectrosc.* **2005**, *59*, 1242.
(14) Kocak, A.; Berets, S. L. *Appl. Spectrosc.* **2008**, *62*, 803.
(15) Hawranek, J. P.; Jones, R. N. *Spectrochim. Acta, Part A* **1976**, *32*, 111.
(16) Hansen, W. N. *Spectrochim. Acta* **1965**, *21*, 815.
(17) Huang, J. B.; Hong, J. W.; Urban, M. W. *Polymer* **1992**, *33*, 5173.

(18) Jackson, M.; Mantsch, H. H. *Appl. Spectrosc.* **1992**, *46*, 699.
(19) Averett, L. A.; Griffiths, P. R.; Hishikida, K. *Anal. Chem.* **2008**, *80*, 3045.
(20) van de Weert, M.; Haris, P. I.; Hennink, W. E.; Crommelin, D. J. A. *Anal. Biochem.* **2001**, *297*, 160.
(21) Hancer, M.; Sperline, R. P.; Miller, J. D. *Appl. Spectrosc.* **2000**, *54*, 138.
(22) Wang, L. Y.; Ding, F.; Zhang, Y. H.; Zhao, L. J.; Hu, Y. A. *Spectrochim. Acta, Part A* **2008**, *71*, 682.
(23) Heavens, O. S. *Optical Properties of Thin Solid Films*; Dover Publications: New York, 1965; p 288.
(24) Azzam, R. M. A.; Bashara, N. M. *Ellipsometry and polarized light*; Library, N.-H. P., Ed.; Elsevier: Amsterdam, The Netherlands, 1977; p 269.
(25) Akai, H. *Experientia* **1983**, *39*, 443.
(26) Holland, C.; Terry, A. E.; Porter, D.; Vollrath, F. *Polymer* **2007**, *48*, 3388.
(27) Mo, C. L.; Holland, C.; Porter, D.; Shao, Z. Z.; Vollrath, F. *Biomacromolecules* **2009**, *10*, 2724.
(28) Asakura, T.; Kuzuhara, A.; Tabeta, R.; Saito, H. *Macromolecules* **1985**, *18*, 1841.
(29) Lefèvre, T.; Boudreault, S.; Cloutier, C.; Pézolet, M. *Biomacromolecules* **2008**, *9*, 2399.
(30) Ohgo, K.; Bagusat, F.; Asakura, T.; Scheler, U. *J. Am. Chem. Soc.* **2008**, *130*, 4182.
(31) Chen, X.; Knight, D. P.; Shao, Z. Z.; Vollrath, F. *Polymer* **2001**, *42*, 9969.
(32) Rousseau, M.-È.; Beaulieu, L.; Lefèvre, T.; Paradis, J.; Asakura, T.; Pézolet, M. *Biomacromolecules* **2006**, *7*, 2512.
(33) Hossain, K. S.; Ochi, A.; Ooyama, E.; Magoshi, J.; Nemoto, N. *Biomacromolecules* **2003**, *4*, 350.
(34) Cameron, D. G.; Kauppinen, J. K.; Moffatt, D. J.; Mantsch, H. H. *Appl. Spectrosc.* **1982**, *36*, 245.
(35) Abeles, F. *Ann. Phys. (Paris)* **1948**, *3*, 504.
(36) Buffeteau, T.; Desbat, B. *Appl. Spectrosc.* **1989**, *43*, 1027.
(37) Yamamoto, K.; Ishida, H. *Appl. Spectrosc.* **1994**, *48*, 775.
(38) Bertie, J. E.; Lan, Z. D. *Appl. Spectrosc.* **1996**, *50*, 1047.
(39) Bardwell, J. A.; Dignam, M. J. *J. Chem. Phys.* **1985**, *83*, 5468.
(40) Blaudez, D.; Boucher, F.; Buffeteau, T.; Desbat, B.; Grandbois, M.; Salesse, C. *Appl. Spectrosc.* **1999**, *53*, 1299.
(41) Buffeteau, T.; Blaudez, D.; Péré, E.; Desbat, B. *J. Phys. Chem. B* **1999**, *103*, 5020.
(42) Buffeteau, T.; Le Calvez, E.; Castano, S.; Desbat, B.; Blaudez, D.; Dufourcq, J. *J. Phys. Chem. B* **2000**, *104*, 4537.
(43) Dignam, M. J. *Appl. Spectrosc. Rev.* **1988**, *24*, 99.
(44) Dignam, M. J.; Mamicheafara, S. *Spectrochim. Acta, Part A* **1988**, *44*, 1435.
(45) Huang, J. B.; Urban, M. W. *Appl. Spectrosc.* **1992**, *46*, 1666.
(46) Iizuka, E. *Biochim. Biophys. Acta* **1968**, *160*, 454.
(47) Goormaghtigh, E.; Cabiaux, V.; Ruysschaert, J. M. Determination of soluble and membranes Protein Structure by Fourier Transform Infrared Spectroscopy III. Secondary Structures In *Physicochemical Methods in the study of Biomembranes*; Hilderson, H. J., Ralston, G. R., Eds.; Plenum Press: New York, 1994; Vol. 23, p 404.
(48) Miyazawa, T.; Blout, E. R. *J. Am. Chem. Soc.* **1961**, *83*, 712.
(49) Young, R. P.; Jones, R. N. *Chem. Rev.* **1971**, *71*, 219.
(50) Tsukada, M.; Freddi, G.; Minoura, N. *J. Appl. Polym. Sci.* **1994**, *51*, 823.
(51) Tsukada, M.; Nagura, M.; Ishikawa, H.; Shiozaki, H. *J. Appl. Polym. Sci.* **1991**, *43*, 643.
(52) Dousseau, F.; Therrien, M.; Pézolet, M. *Appl. Spectrosc.* **1989**, *43*, 538.
(53) Jackson, M.; Mantsch, H. H. *Crit. Rev. Biochem. Mol. Biol.* **1995**, *30*, 95.
(54) Hansen, W. N. *Spectrochim. Acta* **1965**, *21*, 209.

JP101763Y